Electric source imaging of interictal activity accurately localises the seizure onset zone

9 authors, including:

Pierre Mégevand
Hôpitaux Universitaires de Genève
72 PUBLICATIONS **984** CITATIONS

SEE PROFILE

Laurent Spinelli
Hôpitaux Universitaires de Genève
120 PUBLICATIONS **5,831** CITATIONS

SEE PROFILE

Verena Brodbeck
55 PUBLICATIONS **1,973** CITATIONS

SEE PROFILE

Christoph M. Michel
University of Geneva
405 PUBLICATIONS **20,618** CITATIONS

SEE PROFILE

Some of the authors of this publication are also working on these related projects:

Exploring brain communication pathways by combining diffusion based quantitative structural connectivity and EEG source imaging View project

A longitudinal study of school-age children of mothers with interpersonal-violence related PTSD: Understanding effects on the mother-child relationship and child developmental psychopathology View project

Electric source imaging of interictal activity

accurately localises the seizure onset zone

Pierre Mégevand,[1] Laurent Spinelli,[1,2] Mélanie Genetti,[3] Verena Brodbeck,[2,5] Shahan Momjian,[4] Karl Schaller,[4] Christoph M Michel,[2,3] Serge Vulliémoz,[1,2]* Margitta Seeck[1,2]*

(1) EEG and Epilepsy unit, Department of Neurology, Geneva University Hospitals, Switzerland

(2) Department of Clinical Neuroscience, University of Geneva, Switzerland

(3) Department of Fundamental Neuroscience, University of Geneva, Switzerland

(4) Department of Neurosurgery, Geneva University Hospitals, Switzerland

(5) Brain Imaging Center, Department of Neurology, University of Frankfurt a.M., Germany

*equal authorship contribution

Corresponding author: Prof. Margitta Seeck, EEG and Epilepsy Unit, Department of Neurology, Geneva University Hospitals, 4 Rue Gabrielle-Perret-Gentil, 1211 Geneva 14, Switzerland; Margitta.Seeck@hcuge.ch. Phone +41 22 372 83 52. Fax +41 22 372 83 40.

Current address of Pierre Mégevand: Laboratory for Multimodal Human Brain Mapping, Hofstra North Shore-LIJ School of Medicine, Manhasset, NY, USA

Abstract

Objective: It remains controversial whether interictal spikes are a surrogate of the seizure onset zone (SOZ). Electric source imaging (ESI) is an increasingly validated non-invasive approach for localising the epileptogenic focus in patients with drug-resistant epilepsy undergoing evaluation for surgery, using high-density scalp EEG and advanced source localisation algorithms that include the patient's own MRI. Here we investigate if localisation of interictal spikes by ESI provides valuable information on the SOZ.

Methods: In 38 patients with focal epilepsy who later underwent intracranial EEG monitoring, we performed ESI of interictal spikes recorded with 128-256-channel EEG. We measured the distance between the ESI maximum and the nearest intracranial electrodes in the SOZ and irritative zone (IZ, the source of interictal spikes). The resection of the region harbouring the ESI maximum was correlated to surgical outcome.

Results: The median distance from the ESI maximum to the nearest electrode involved in the SOZ was 17 mm (interquartile range 8-27). The IZ and SOZ co-localised in most patients (median distance 0 mm, interquartile range 0-14), supporting the notion that localising interictal spikes is a valid surrogate for the seizure onset zone. There was no difference in accuracy among patients with temporal or extra-temporal epilepsy. In the 32 patients who underwent resective surgery, including the ESI maximum in the resection correlated with favourable outcome (p=0.03).

Conclusions: Localisation of interictal spikes provides an excellent estimate of the SOZ in the majority of patients. ESI should be taken into account for the management of patients undergoing intracranial recordings.

INTRODUCTION

Surgical resection of the epileptogenic zone is a therapeutic option for patients suffering from drug-resistant focal epilepsy, leading to seizure freedom in a substantial proportion of cases.[1] In order to maximise the chances of seizure freedom and minimise the risk of neurological deficit, the cortical area responsible for seizure generation must be localised as accurately as possible. Intracranial EEG of the seizure onset zone is the gold standard for this purpose.[2] However, because intracranial EEG is invasive and cannot sample the activity from the whole brain, non-invasive approaches play a capital role in selecting patients and designing the implantation strategy.[3]

EEG-based electric source imaging (ESI) directly estimates the cerebral generators of surface-recorded electric fields.[4-8] Using high-density EEG systems, head models that take into account the cerebral anatomy of the individual patient, and distributed inverse solutions, ESI of interictal spikes is among the most accurate non-invasive approaches for localising the epileptogenic zone, as validated by the concordance of ESI with the resected brain volume and surgical outcome.[9]

Despite these recent progresses, uncertainty persists on two issues. First, it still remains controversial whether the irritative zone (IZ), which produces interictal spikes, co-localises with the seizure onset zone (SOZ).[5] If high-definition ESI of interictal spikes localises the underlying source reliably, and if the IZ is a valuable surrogate for the SOZ, then ESI should identify the SOZ. So far, no study has compared ESI of interictal spikes to the localisation of the SOZ by intracranial EEG. Second, in epilepsy surgery, the resection generally involves a larger

volume than just the seizure onset zone and may include non-epileptogenic tissue so that the exact concordance between ESI and the epileptic generators cannot be formally determined from post-operative comparisons alone. In the present study, we set out to compare ESI of interictal spikes to the localisation of the SOZ by intracranial EEG in a cohort of 38 patients with focal epilepsy, assessing the spatial accuracy of ESI on a subcentimetric scale.

METHODS

Patients

This study was approved by the institutional ethical review committee of Geneva University Hospitals. Patients gave their written consent to participate. Between 2000 and 2011, we prospectively recruited 44 consecutive patients with drug-resistant epilepsy who had undergone high-density EEG recordings with at least 128 channels prior to intracranial video-EEG monitoring at the epilepsy unit of Geneva University Hospitals, Switzerland. High-density EEG failed to record epileptic activity in 6 patients (14%). Thus, 38 patients (17 females) were studied further (supplementary table 1). Nineteen (50%) had temporal lobe epilepsy (TLE; 14 medial (MTLE), 5 lateral (LTLE)) and 19 (50%) extra-temporal lobe epilepsy (ETLE). Patients with temporal polar epilepsy were classified in the MTLE group. Median age at evaluation was 24 years (range 3-51); median age at epilepsy onset was 10 years (range 0-33).

EEG recordings, spike selection and averaging

All patients underwent a comprehensive non-invasive evaluation, including neurological, neuropsychological and psychiatric examinations, 32-channel long-term video-EEG monitoring,

3D millimetric MRI, PET. Subtraction ictal-interictal SPECT co-registered with MRI (SISCOM) was performed in 35 patients.

High-density EEG was recorded for 30 to 60 minutes using 128- or 256-electrode Geodesic Sensor Nets® (Electrical Geodesics Inc., Eugene, OR), as previously described.[9] Impedances were kept below 20 kOhm. EEG was filtered (0.1-100 Hz) and digitized at 256-1000-Hz sampling rate with a vertex electrode as reference. A neurologist experienced in clinical EEG (VB, SV, MS) marked all spike peaks that were then averaged within a window of 500 ms pre- and post-spike. In cases where more than one spike with different surface topographies were recorded (n=9), only the most frequent topography was retained for further analysis. Artefact-ridden channels were removed and interpolated.

Head model and inverse solution

To compute the forward model, we used a head model based on the individual patient's T1-weighted 3D millimetric MRI. The brain surface was extracted from this MRI and the best-fitting sphere was calculated. The MRI was then warped according to the ratio of the sphere radius and the real surface radius. Depending on brain size, between 3000 and 5000 solution points were defined at regular distances within the grey matter including deep structures such as the amygdala and the hippocampus.[10] The lead field matrix was then computed using the known analytical solutions for a 3-shell spherical head model with a conductivity ratio of 1:20 between skull and brain.[11, 12] A linear distributed inverse solution with biophysical constraints was used to calculate the 3D current density distribution.[13] Finally, the result was back-transformed to the original head shape. This simplified anatomically constrained head model was shown to

reveal similar localizations as a boundary element model.[14] The localisation of the solution point with the maximal source amplitude at 50% of the rising phase of the spike was considered for subsequent analysis (ESI maximum). This time point most reliably localises the underlying electrical source, whereas the localisation at the peak of the spike is contaminated by spike propagation.[15-17] When we observed rhythmic spike discharges or very close consecutive spikes, only the first spike was analysed. EEG and ESI analyses were performed using the free Cartool software (http://brainmapping.unige.ch/cartool).[18]

Intracranial EEG

Grids and strips of subdural electrodes (in 13 patients), depth electrodes (in 12 patients), or combinations of both (in 13) were implanted (range 38 to 128 electrodes) according to the individual non-invasive presurgical work-up (supplementary table 1). Intracranial electrodes were localised on a post-implantation CT scan and co-registered with the pre-implantation MRI using Analyze 9 (Biomedical Imaging Resource, Mayo Clinic, Rochester, MN). To compensate for the brain shift caused by subdural electrode implantation, these electrodes were projected back orthogonally to the brain surface of the pre-implantation MRI.

Interictal spikes and seizures recorded with intracranial EEG were reviewed by board-certified neurologists and neurophysiologists with additional experience in intracranial EEG (SV, MS). Electrodes displaying interictal spikes formed the irritative zone (IZ). Likewise, electrodes displaying the earliest ictal activity formed the seizure onset zone (SOZ).[19] Contacts involved only in the propagation of interictal spikes or seizures were not included in the IZ or SOZ.

Surgery

Following intracranial video-EEG monitoring, surgery was carried out in 32/38 patients (84%).

Follow-up was at least 1 year. Outcome was more favourable for patients with TLE (10/15, 67%,

were Engel class I, i.e. seizure-free) than for those with ETLE (5/17, 29%; chi-square=4.4414,

p=0.0351).

Distance measurement

Euclidian distances were measured between the ESI maximum and the nearest intracranial

electrodes involved in the IZ and the SOZ. The frequency of intracranial spikes was not a

criterion in deciding which intracranial spike corresponded to the scalp spike. The fact that

subdural electrodes lie at the surface of the brain over the gyral crowns spuriously increases the

ESI-electrode distance if the ESI maximum is in fact buried in the depth of a sulcus. Therefore,

when subdural electrodes were used, we corrected for this depth error by orthogonally projecting

the ESI maximum onto the brain surface.

In the patients who underwent surgery, we measured the distance between the ESI maximum and

the resection cavity on a post-operative MRI (or CT in 2 cases) co-registered to the pre-operative

MRI. ESI was considered concordant with the resection when the solution point with the ESI

maximum was located within or on the margin of the resection revealed by post-operative

imaging. A solution point was on the margin of the resection when one of its direct neighbours

was inside the resection.

Statistical analysis

We used the chi-square test to evaluate differences between proportions, the Wilcoxon rank sum test to compare differences between distributions, and the Spearman rank correlation coefficient to assess the significance of correlations. Graphical data representation and statistical analysis were performed using MATLAB 9 with the Statistics Toolbox (MathWorks, Natick, MA). Values of $p \leq 0.05$ were considered significant.

RESULTS

Electric source imaging of interictal spikes and the seizure onset zone

The ESI-SOZ distance in a given patient is determined by (1) the accuracy of ESI in localising the source of interictal spikes (the ESI-IZ distance), and (2) the degree to which the IZ overlaps with the SOZ (the IZ-SOZ distance). The median distance between the ESI maximum and the nearest IZ electrode was 15 mm (interquartile range 8-21; figure 1A). The distribution of ESI-IZ distances appeared unimodal, with the distances being smaller than 30 mm in all but one outlying patient and smaller than 20 mm in 71% of patients.

The median distance between the IZ and SOZ electrodes nearest the ESI maximum was 0 mm (interquartile range 0-14). The IZ and SOZ electrodes nearest the ESI maximum were the same electrode in 21/38 patients (55%).

The median distance between the ESI maximum and the nearest electrode involved in the SOZ was 17 mm (interquartile range 8-27; figure 1C). The distribution of ESI-SOZ distances was

bimodal, with most distances (87%) being smaller than 35 mm. Figure 2A-C illustrates successful localisation of the SOZ by ESI.

Patients with discordant localisation of IZ and SOZ

Examining the 5 patients with the largest ESI-SOZ distances, we found that they all had ESI-IZ distances comparable to those of the other patients (see figure 1B). In these patients, all with multifocal irritative zones, the ESI in fact accurately localised a part of the IZ, but that IZ was not part of the SOZ. Only one spike topography was recorded during high-density scalp EEG in these patients. In Patient 1 (patient numbers refer to supplementary table 1), the ESI localised a right inferior frontal IZ, whereas the SOZ lay in the right medial temporal lobe. In Patient 7 (figure 2D), the ESI localised a left temporo-parietal IZ concordant with clinical video-EEG and PET results, whereas the SOZ was in the left basal temporal lobe. Patient 4 had bilateral temporal irritative zones in clinical scalp and intracranial EEG but only left-sided spikes were captured during the high-density EEG recording. The ESI identified a left temporal IZ, whereas the SOZ lay in the right temporal lobe. Similarly, Patient 38 had bilateral frontal irritative zones, but ESI only characterised the left frontal IZ whereas the SOZ was located in the right frontal lobe. Finally, Patient 32 had a left frontal periventricular heterotopia from where both spikes and seizures originated. However, the head model did not allow for isolated solution points to be placed in the small heterotopia and the ESI could therefore technically not be located there. It lay instead in the left middle frontal gyrus which showed propagation from the spikes generated in the periventricular nodular heterotopia. In 4 of these 5 patients, surgery either was not offered or did not bring persistent seizure freedom, illustrating the complex nature of their epileptic networks.

ESI and epilepsy subtype

Comparing patients with TLE and ETLE, we found no significant differences in the ESI-SOZ distance (Wilcoxon rank sum statistic W=413, p=0.2201, 2-tailed). There were also no significant differences when comparing patients with medial TLE versus neocortical epilepsies (LTLE and ETLE) (W=312, p=0.244, 2-tailed). Finally, we found no significant difference between patients with medial and lateral TLE (W=45, p=0.6868). Hence, ESI did not appear to perform better in any epilepsy subtype, although the small number of patients with LTLE (n=5) calls for caution in interpreting this comparison.

ESI and postoperative outcome

In the 32 patients who underwent resective surgery, the ESI maximum lay within the resection significantly more often in patients who became seizure-free (Engel class I outcome: 12/15 patients, 80%) than in those with less favourable outcomes (7/17 patients, 41%; chi-square=4.9795, p=0.0256). This suggests that careful analysis of interictal spikes is useful in delineating the epileptogenic zone.

Outcomes in the patients in whom more than one spike topography was recorded during high-density EEG (n=9) were not different from those of patients with a single spike topography. Among the patients in whom the ESI-SOZ distance was less than 10 mm (n=11), the outcome was Engel class I in 6 and class III or IV in 3 (2 patients did not undergo resective surgery).

DISCUSSION

In this study, we evaluated the accuracy of electric source imaging of interictal spikes in delineating the seizure onset zone defined by intracranial EEG. Our main finding is that the localisation of interictal spikes by ESI in the individual patient's own MRI provides an accurate estimate of the seizure onset zone. Furthermore, including the source maximum in the resected brain volume is associated with a favourable post-operative outcome, indicating that ESI of interictal spikes helps delineating the epileptogenic zone. Importantly, ESI performs similarly well in temporal and extratemporal epilepsy. These results bolster the role of ESI of interictal spikes as a reliable tool to delineate the seizure onset zone and add to the evidence that ESI has an important role to play in defining the strategy both for the implantation of intracranial electrodes and for resective surgery.

As mentioned earlier, no study that we know of has compared ESI of interictal spikes to intracranial EEG localisation of the SOZ. A magnetoencephalographic source imaging study of interictal spikes found co-localisation with the SOZ at a sub-lobar level in 78% of cases of LTLE and 45% of cases of MTLE and ETLE.[20, 21] Comparing these encouraging results with ours is not straightforward, because sub-lobar regions are defined according to anatomical landmarks and can differ widely in size and shape. We estimated the average size of a sub-lobar region: the total surface of one cerebral hemisphere is 820 cm^2, two thirds of which are buried in sulci.[22] Its outer surface is therefore about 270 cm^2. Parcellating this surface into 13 circles of equal area (the number of regions per hemisphere used by Knowlton et al. [20, 21]) yields regions with a radius of about 25 mm. In our study, 71% of ESI-SOZ distances were below 25 mm, a performance that compares favourably to the aforementioned study.

Successful epilepsy surgery by definition entails resecting the entire epileptogenic zone.[2] However, because this zone cannot be defined unambiguously before surgery, the IZ and SOZ must be used as surrogates in clinical practice. Of these, the SOZ is often considered to be the better one,[23] but the vast majority of non-invasive localising techniques are based on interictal activity, as seizures can generally only be recorded serendipitously or with long-term recordings and are frequently accompanied by motion artefacts. Our finding that the IZ co-localised with the SOZ in most cases is in line with previous research and affects not only ESI, but also magnetic source imaging (MSI) or EEG-fMRI.[16, 24, 25] In addition, including the ESI maximum in the resection volume was associated with a favourable post-operative outcome, confirming our previous findings.[9] Similarly good prognostic performance was also found with MSI.[26] The clinical importance of delineating the IZ in addition to the SOZ is also underlined by findings that patients whose SOZ is completely contained in the resected brain volume, but whose IZ extends beyond the margins of the surgical resection, had poorer surgical outcome.[27] The peri-lesional primary irritative zone (but not remote interictal generators) might be a better surrogate of the epileptogenic zone than a very focal SOZ corresponding to only a subset of the epileptic network.

In a minority of our patients, ESI localised an IZ that was not part of the SOZ as revealed by intracranial EEG.[28] These patients all had complex epileptic networks with multifocal, sometimes bi-hemispheric irritative zones and poorer outcome if operated. As it is true of any investigation, ESI should not be interpreted in isolation, but must be integrated within the complete clinical, electrophysiological and neuroimaging picture for optimal management.

Recording high-density EEG for longer periods of time, including during sleep, will likely increase the yield of ESI and the detection of multifocal activity. Further, imaging the source of each spike topography may help planning the implantation of intracranial electrodes in order to better sample the complex, multifocal networks generating spikes and seizures.

In our study, the accuracy of ESI was limited by the following methodological considerations. Its spatial resolution is limited by the distance between neighbouring solution points (about 5 mm in each anatomical plane). Additionally, we restricted our analysis of ESI results to the point of maximum intensity, not taking into account the spatial spread of the source analysis for which there is currently no established algorithm. Furthermore, intracranial EEG is an imperfect gold standard: its spatial sampling (the areas of the brain recorded by the intracranial electrodes) is always partial and its spatial resolution is rather in the range of 5-10 mm, so that the epileptogenic zone may be missed (e.g. if it is buried in a deep sulcus).[21] This is illustrated in our patients by the fact that a short ESI-SOZ distance was not unequivocally related to an excellent post-operative outcome. Keeping these limitations in mind, ESI-IZ and ESI-SOZ distances of 20 mm or below, as observed in the majority of our patients, can be considered very accurate.

An open question in electric and magnetic source imaging pertains to identifying the surface counterparts of intracranial EEG spikes, and particularly whether spikes generated by and confined to the medial temporal lobe can be recorded at the scalp surface. Probably the best way of tackling this issue is to compare simultaneously recorded scalp EEG or MEG with intracranial EEG.[5] Studies which applied this methodology to small patient numbers yielded conflicting

results: some found that a fraction of medial temporal spikes are visible at the scalp surface [29-31] while others did not.[32] Further research using simultaneous scalp and intracranial recordings in larger patient cohorts will be necessary to better address this important point. A related concern is the possibility that the rapid propagation of spikes away from their initial generators towards distant brain regions [16, 17] might lead to erroneous electromagnetic source imaging results. ESI performed on the initial rising phase of spikes strongly reduces such contamination.[15] Here as well, simultaneous scalp and intracranial EEG recordings will be helpful in understanding how spike propagation can affect the performance of ESI.

Our study illustrates that ESI of interictal epileptic spikes provides an accurate estimate of the seizure onset and epileptogenic zones. We suggest that the accuracy of ESI is sufficient to influence surgical decision-making in patients with drug-resistant epilepsy undergoing pre-surgical evaluation, similarly to findings obtained with MSI.[3, 33, 34] ESI performs similarly well in patients with temporal or extra-temporal lobe epilepsy. The ease of use of current high-density EEG systems (bedside recording, no sedation required, feasible in young children and cognitively impaired patients) should increase the availability of ESI. This validation of ESI is also informative for other applications of the technique, both in clinical neurology for localising and testing the function of sensory, motor and cognitive cortical areas as well as in cognitive neuroscience.[35, 36] Finally, our findings give support and clinical relevance to other techniques which use interictal epileptogenic discharges to identify the seizure onset zone, such as MEG and simultaneous EEG-fMRI.[4, 37]

Contributors

- PM: study design, data collection and analysis, drafting the manuscript, preparing the figures.

- LS: study design, data collection and analysis.

- MG: data collection and analysis.

- VB: data collection and analysis.

- SM: data collection and analysis.

- KS: study design, data analysis.

- CMM: study design, data analysis, drafting the manuscript.

- SV: study design, data collection and analysis, drafting the manuscript.

- MS: study design, data collection and analysis, drafting the manuscript.

- All authors reviewed the manuscript and approved the final version.

Competing interests

- PM, LS, MG, VB, SM, and KS report no competing interests.

- CMM receives honoraria from Springer as editor-in-chief of *Brain Topography*, and receives royalties from Cambridge University Press as one of the editors of the book *Electrical Neuroimaging*.

- SV received speaker's fees from Electrical Geodesics, Inc., for an invited lecture in an industry symposium, and serves as a consultant in advisory boards for Eisai Pharmaceuticals and Desitin Pharma.

- MS has received speaker's fees from Electrical Geodesics, Inc., for an invited lecture in an industry symposium, and serves as a consultant in advisory boards for Eisai Pharmaceuticals, UCB Pharma, and GlaxoSmithKline.

- Electrical Geodesics, Inc., the company that manufactures some of the equipment used to acquire high-density EEG in this study, played no role in study design, data collection and analysis, or in writing and submission of the paper.

Ethics approval

This study was approved by the institutional ethical review committee of Geneva University Hospitals.

REFERENCES

1. Spencer S, Huh L. Outcomes of epilepsy surgery in adults and children. Lancet Neurol 2008;**7**(6):525-37 doi: 10.1016/S1474-4422(08)70109-1.

2. Rosenow F, Lüders H. Presurgical evaluation of epilepsy. Brain 2001;**124**(9):1683-700 doi: 10.1093/brain/124.9.1683.

3. Knowlton RC, Razdan SN, Limdi N, et al. Effect of epilepsy magnetic source imaging on intracranial electrode placement. Ann Neurol 2009;**65**(6):716-23 doi: 10.1002/ana.21660.

4. Grouiller F, Thornton RC, Groening K, et al. With or without spikes: localization of focal epileptic activity by simultaneous electroencephalography and functional magnetic resonance imaging. Brain 2011;**134**(Pt 10):2867-86 doi: 10.1093/brain/awr156.

5. Kaiboriboon K, Luders HO, Hamaneh M, et al. EEG source imaging in epilepsy--practicalities and pitfalls. Nat Rev Neurol 2012;**8**(9):498-507 doi: 10.1038/nrneurol.2012.150.

6. Michel CM, Murray MM. Towards the utilization of EEG as a brain imaging tool. Neuroimage 2012;**61**(2):371-85 doi: 10.1016/j.neuroimage.2011.12.039.

7. Michel CM, Murray MM, Lantz G, et al. EEG source imaging. Clin Neurophysiol 2004;**115**(10):2195-222 doi: 10.1016/j.clinph.2004.06.001.

8. Plummer C, Harvey AS, Cook M. EEG source localization in focal epilepsy: where are we now? Epilepsia 2008;**49**(2):201-18 doi: 10.1111/j.1528-1167.2007.01381.x.

9. Brodbeck V, Spinelli L, Lascano AM, et al. Electroencephalographic source imaging: a prospective study of 152 operated epileptic patients. Brain 2011;**134**(Pt 10):2887-97 doi: 10.1093/brain/awr243.

10. Spinelli L, Andino SG, Lantz G, et al. Electromagnetic inverse solutions in anatomically constrained spherical head models. Brain Topogr 2000;**13**(2):115-25 doi: 10.1023/A:1026607118642.

11. Ary JP, Klein SA, Fender DH. Location of sources of evoked scalp potentials: corrections for skull and scalp thicknesses. IEEE Trans Biomed Eng 1981;**28**(6):447-52 doi: 10.1109/tbme.1981.324817.

12. Goncalves S, de Munck JC, Verbunt JP, et al. In vivo measurement of the brain and skull resistivities using an EIT-based method and the combined analysis of SEF/SEP data. IEEE Trans Biomed Eng 2003;**50**(9):1124-8 doi: 10.1109/tbme.2003.816072.

13. Grave de Peralta Menendez R, Murray MM, Michel CM, et al. Electrical neuroimaging based on biophysical constraints. Neuroimage 2004;**21**(2):527-39 doi: 10.1016/j.neuroimage.2003.09.051.

14. Guggisberg AG, Dalal SS, Zumer JM, et al. Localization of cortico-peripheral coherence with electroencephalography. NeuroImage 2011;**57**(4):1348-57 doi: 10.1016/j.neuroimage.2011.05.076.

15. Lantz G, Spinelli L, Seeck M, et al. Propagation of Interictal Epileptiform Activity Can Lead to Erroneous Source Localizations: A 128-Channel EEG Mapping Study. Journal of Clinical Neurophysiology 2003;**20**(5):311-19.

16. Ray A, Tao JX, Hawes-Ebersole SM, et al. Localizing value of scalp EEG spikes: a simultaneous scalp and intracranial study. Clin Neurophysiol 2007;**118**(1):69-79 doi: 10.1016/j.clinph.2006.09.010.

17. Alarcon G, Guy CN, Binnie CD, et al. Intracerebral propagation of interictal activity in partial epilepsy: implications for source localisation. J Neurol Neurosurg Psychiatry 1994;**57**(4):435-49.

18. Brunet D, Murray MM, Michel CM. Spatiotemporal analysis of multichannel EEG: CARTOOL. Comput Intell Neurosci 2011;**2011**:813870 doi: 10.1155/2011/813870.

19. Seeck M, Schomer DL, Niedermeyer E. Intracranial Monitoring: Depth, Subdural and Foramen Ovale Electrodes. In: Schomer DL, Lopes Da Silva FH, eds. Niedermeyer's Electroencephalography--Basic Principles, Clinical Applications and Related Fields. Philadelphia, PA: Lippincott Williams Wilkins, 2011:677-714.

20. Knowlton RC, Elgavish RA, Bartolucci A, et al. Functional imaging: II. Prediction of epilepsy surgery outcome. Ann Neurol 2008;**64**(1):35-41 doi: 10.1002/ana.21419.

21. Knowlton RC, Elgavish RA, Limdi N, et al. Functional imaging: I. Relative predictive value of intracranial electroencephalography. Ann Neurol 2008;**64**(1):25-34 doi: 10.1002/ana.21389.

22. Henery CC, Mayhew TM. The cerebrum and cerebellum of the fixed human brain: efficient and unbiased estimates of volumes and cortical surface areas. J Anat 1989;**167**:167-80.

23. Marsh ED, Peltzer B, Brown MW, 3rd, et al. Interictal EEG spikes identify the region of electrographic seizure onset in some, but not all, pediatric epilepsy patients. Epilepsia 2010;**51**(4):592-601 doi: 10.1111/j.1528-1167.2009.02306.x.

24. Asano E, Muzik O, Shah A, et al. Quantitative interictal subdural EEG analyses in children with neocortical epilepsy. Epilepsia 2003;**44**(3):425-34 doi: 10.1046/j.1528-1157.2003.38902.x.

25. Hufnagel A, Dumpelmann M, Zentner J, et al. Clinical relevance of quantified intracranial interictal spike activity in presurgical evaluation of epilepsy. Epilepsia 2000;**41**(4):467-78 doi: 10.1111/j.1528-1157.2000.tb00191.x.

26. Fischer MJ, Scheler G, Stefan H. Utilization of magnetoencephalography results to obtain favourable outcomes in epilepsy surgery. Brain 2005;**128**(Pt 1):153-7 doi: 10.1093/brain/awh333.

27. Bautista RE, Cobbs MA, Spencer DD, et al. Prediction of surgical outcome by interictal epileptiform abnormalities during intracranial EEG monitoring in patients with extrahippocampal seizures. Epilepsia 1999;**40**(7):880-90 doi: 10.1111/j.1528-1157.1999.tb00794.x.

28. Bettus G, Ranjeva JP, Wendling F, et al. Interictal functional connectivity of human epileptic networks assessed by intracerebral EEG and BOLD signal fluctuations. PLoS One 2011;**6**(5):e20071 doi: 10.1371/journal.pone.0020071.

29. Lantz G, Grave de Peralta Menendez R, Gonzalez Andino S, et al. Noninvasive localization of electromagnetic epileptic activity. II. Demonstration of sublobar accuracy in patients with simultaneous surface and depth recordings. Brain Topogr 2001;**14**(2):139-47.

30. Yamazaki M, Tucker DM, Fujimoto A, et al. Comparison of dense array EEG with simultaneous intracranial EEG for interictal spike detection and localization. Epilepsy Res 2012;**98**(2-3):166-73 doi: 10.1016/j.eplepsyres.2011.09.007.

31. Zumsteg D, Friedman A, Wennberg RA, et al. Source localization of mesial temporal interictal epileptiform discharges: correlation with intracranial foramen ovale electrode recordings. Clin Neurophysiol 2005;**116**(12):2810-8 doi: 10.1016/j.clinph.2005.08.009.

32. Wennberg R, Valiante T, Cheyne D. EEG and MEG in mesial temporal lobe epilepsy: where do the spikes really come from? Clin Neurophysiol 2011;**122**(7):1295-313 doi: 10.1016/j.clinph.2010.11.019.

33. De Tiege X, Carrette E, Legros B, et al. Clinical added value of magnetic source imaging in the presurgical evaluation of refractory focal epilepsy. J Neurol Neurosurg Psychiatry 2012;**83**(4):417-23 doi: 10.1136/jnnp-2011-301166.

34. Sutherling WW, Mamelak AN, Thyerlei D, et al. Influence of magnetic source imaging for planning intracranial EEG in epilepsy. Neurology 2008;**71**(13):990-6 doi: 10.1212/01.wnl.0000326591.29858.1a.

35. Lascano AM, Brodbeck V, Lalive PH, et al. Increasing the diagnostic value of evoked potentials in multiple sclerosis by quantitative topographic analysis of multichannel recordings. J Clin Neurophysiol 2009;**26**(5):316-25 doi: 10.1097/WNP.0b013e3181baac00.

36. Laganaro M, Morand S, Michel CM, et al. ERP correlates of word production before and after stroke in an aphasic patient. J Cogn Neurosci 2011;**23**(2):374-81 doi: 10.1162/jocn.2010.21412.

37. Vulliemoz S, Lemieux L, Daunizeau J, et al. The combination of EEG Source Imaging and EEG-correlated functional MRI to map epileptic networks. Epilepsia 2010;**51**(4):491-505.

Supplementary table 1. Clinical characteristics of the patients

Supplementary table 1 is provided as an Adobe PDF file.

Abbreviations: L=left, R=right, bilat=bilateral, F=frontal, C=central, T=temporal, P=parietal, O=occipital, ant=anterior, post=posterior, sup=superior, inf=inferior, lat=lateral, Hipp=hippocampus, parahipp=para-hippocampal gyrus, Amyg=amygdala, Forb=frontal orbital, Cing=cingular, SMA=supplementary motor area, HS=hippocampal sclerosis, ATLR=anterior temporal lobe resection, MTLE=medial temporal lobe epilepsy, LTLE=lateral temporal lobe epilepsy, ETLE=extra-temporal lobe epilepsy.

Legends of Figures

Figure 1. Accuracy of ESI in localising the irritative zone (IZ) and the seizure onset zone (SOZ)

(A) The distances between the ESI maximum and the nearest IZ electrode are displayed as a histogram. N: number of patients. Please refer to figure 1B for the legends to the colours of the histogram bars.

(B) For each patient, the distance between the ESI maximum and the nearest SOZ electrode is plotted against the ESI-IZ distance. In most patients, these two distances were very similar to each other (points are near the diagonal line of identity). The colours of the points indicate the epilepsy subtype (MTLE: medial temporal lobe epilepsy; LTLE: lateral temporal lobe epilepsy; ETLE: extratemporal lobe epilepsy).

(C) The ESI-SOZ distances are displayed as a histogram.

Figure 2. Examples of ESI localisation

In this Figure, the ESI maximum is marked as a red cross, the nearest IZ electrode as a white circle, and the nearest SOZ electrode as a blue circle. When the nearest IZ and SOZ electrodes coincide, the electrode is marked as a half-blue, half-white circle.

(A) Patient 33, ETLE: successful ESI localisation. Engel class I.

(B) Patient 14, MTLE: successful ESI localisation. Engel class I. The left side of the patient is displayed on the right side of the image according to radiological convention.

(C) Patient 30, ETLE: successful ESI localisation. Engel class I.

(D) Patient 7, MTLE: unsuccessful ESI localisation of the SOZ despite successful localisation of the IZ. The ESI (red cross) lay in the left angular gyrus, close to an IZ electrode that was not part of the SOZ (white circle). The SOZ lay in the basal temporal lobe (blue circle). Engel class II.
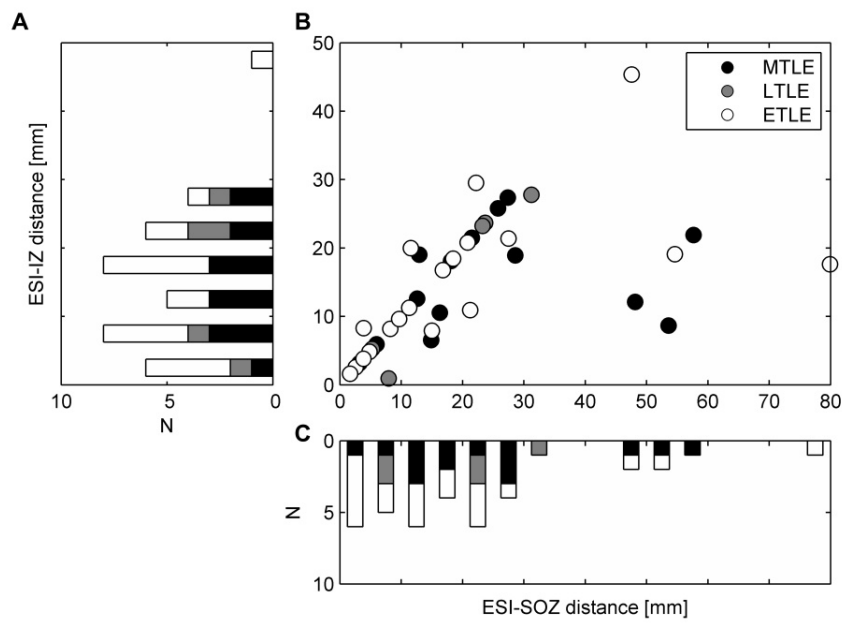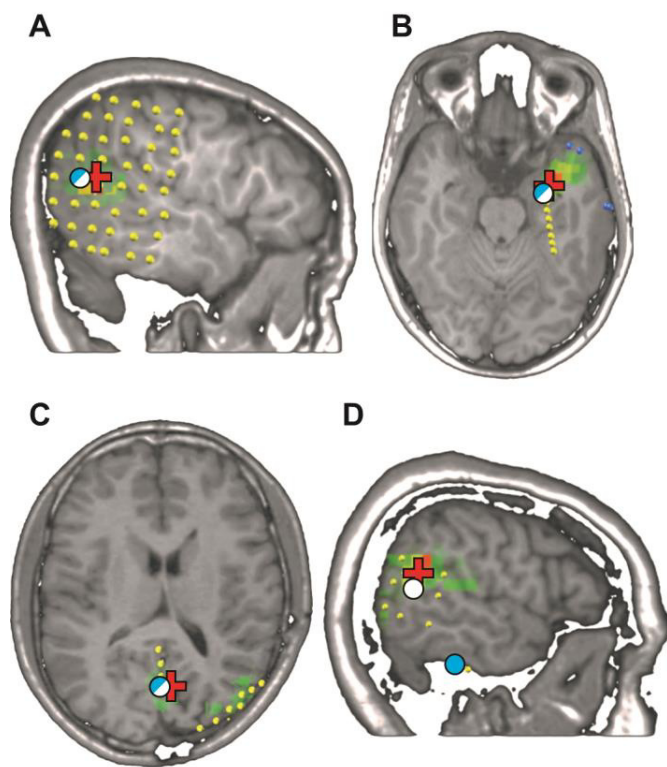
Figure 1

Figure 2

Accuracy of Electric Source Imaging in epilepsy

Supplementary Table 1

#	Gender	Age at evaluation	Age at onset	Classification	MRI findings	Surface spikes	ESI result	iceEEG setup	icEEG spikes	icEEG seizure onsets	Surgery	Engel class
1	M	16	11	MTLE	R HS	R F-T	R inf F gyrus (pars orbitalis)	depth R Amyg, R Hipp, R Forb, R Cing, L Hipp	R Amyg and Hipp > R Forb	R Amyg and Hipp	R ATLR	1
2	M	32	18	MTLE	L Hipp cyst (uncertain significance)	L T > L F-C	L mid T gyrus	depth left Cing, left Forb, left SMA, left Amyg, left Hipp ant, left Hipp post	L Amyg and Hipp > L F ant	L Amyg and Hipp	L ATLR	1
3	M	46	21	MTLE	R HS, R F nodular periventricular heterotopia	L T	R Amyg	depth R F, bilat Amyg, Hipp ant, Hipp post, Cing, Forb	R T lat ant > R Hipp > L Hipp	R Hipp and Amyg	R ATLR	1
4	M	45	21	MTLE	gliosis L P	R T = L T	L sup T gyrus (polar)	depth bilat Forb, Cing, SMA, Amyg, Hipp ant, Hipp post	R Hipp ant = L Hipp ant > R Amyg = L Amyg	R Amyg	NO	N/A
5	F	32	9	MTLE	R HS	R T > L T > F bilat	R Amyg	depth R Forb, R insula, R amygdala, bilat Cing, bilat Hipp	R Hipp > L Hipp	R Hipp	R amygdalo-hippocampectomy	1
6	F	43	33	MTLE	L Hipp atrophy (uncertain significance)	R T	R Amyg	grid R T-P-F, strips R T ant, R T basal	R T ant	R T ant medial	R T lobectomy	2
7	F	39	16	MTLE	Mild L hemisphere atrophy (uncertain significance)	L T	L angular gyrus	grid L F-P-T, strips L F, L T basal, L P	L T polar and medial > L T inf lat > L T basal > L P	L T polar and medial	L T lobectomy and P basal cortectomy	2
8	M	28	21	MTLE	R T and P nodular periventricular heterotopia, R T cortical dysplasia	R T > F bilat	R mid T gyrus-inf T sulcus	depth R Amyg, R Hipp, R P heterotopia, L Hipp, bilat Forb, bilat Cing	R T heterotopia > L Hipp	R T heterotopia	R T lesionectomy	1
9	M	29	18	MTLE	bilat T periventricular heterotopia	R T > L T	R inf T gyrus (post)	depth bilat Amyg, Hipp, heterotopia	(wake) R Hipp and Amyg (sleep) L Hipp and Amyg	(typical) L Hipp and Amyg (atypical) R T post lat	NO	N/A
10	F	28	14	MTLE	normal	R T	R sup T gyrus (polar)	depth bilat Amyg, bilat Hipp, R Forb, R Cing	R Hipp and Amyg > L Hipp and Amyg > R T lat ant	R Hipp	R ATLR	1
11	M	34	15	MTLE	normal, DBS electrode L Hipp	L T	L Hipp	grid L F-P-T, strips L T polar, L T basal, L O, depth L Hipp	L Hipp > L T basal > L O > L F	(clinical) L Hipp (subclinical) L T lat	L T polectomy	3
12	F	34	13	MTLE	L HS, R T lobar atrophy	L T > R T	L mid T gyrus (polar)	depth bilat Amyg, Hipp, Cing, Forb	(wake) L Hipp > (sleep) R Hipp and Amyg	L Hipp	L amygdalo-hippocampectomy	2
13	F	31	25	MTLE	normal	L T > R T	L Hipp, Amyg	depth bilat Amyg, Hipp, Cing, Forb	L Hipp > R Hipp and Amyg	L Hipp > R Hipp and Amyg	NO	N/A
14	M	18	8	MTLE	L T polar size reduction (uncertain significance)	L T > R T	L Hipp, Amyg	grid L F-T, depth bilat Hipp, strips L F basal, L insula, L T basal	L T basal > L Hipp	L T basal ant	L ATLR	1
15	M	34	14	LTLE	possible L parahipp dysplasia	L T-O	L sup O gyrus	grid L T-P-O, depth L parahipp, L Hipp	L T-O > L Hipp	L T-O	NO	N/A
16	M	18	13	LTLE	normal	L T > R T	L sup T gyrus (polar)	depth bilat Amyg, bilat Hipp, left Forb, L F lat	L T lat ant > R T lat > L F basal > L F lat	L T lat ant	L ATLR sparing medial T structures	1
17	M	11	8	LTLE	R T porencephaly, periventricular gliosis	R P-O > R T > R F-T	R supramarginal gyrus	grid R P-T-F, depth bilat Hipp, right Amyg, right Forb	R T sup post-P > R T inf lat > R T lat ant > L Hipp = R Amyg	R T sup post-P	R T-P cortectomy	3
18	M	12	1	LTLE	tuberous sclerosis	L T > L F > R F > L T-P	L mid T gyrus-sup T sulcus	grid L T-P-F, strips L F ant, L T lat ant, L T basal, L T polar, depth bilat Forb, R Hipp	L T basal	L T polar	L T lobectomy	1
19	F	22	7	LTLE	L T post dysplasia	L T > R T	L Hipp, Amyg	grid L T-F-P, grid L P-O, strips L F basal, L T basal	L T lat sup > L T basal > L P-O	L T lat sup	L T lobectomy	1
20	F	9	3	ETLE	normal	C-P midline	L supramarginal gyrus-intraparietal sulcus	grid L P-F-T, strips L F-P medial	L P medial > L P sup	L P sup	R P parasagittal cortectomy	4
21	F	12	1	ETLE	tuberous sclerosis	L C = L F	L mid F gyrus	grid L T-P, depth L F, L T-P	L F post > L F ant	L F ant	Tuber resection L F ant, L C	1
22	M	11	1	ETLE	resection L F dysplasia	L F > L T	L sup T gyrus	grid L F-T-P, strips L F-P medial, L T polar, depth L Hipp, L insula	L F operculum-insula	L F operculum-insula	R F opercular-insular-T polar resection	1
23	M	14	1	ETLE	normal	R F-C	R mid F gyrus-precentral sulcus	grid R F, depth bilat SMA, bilat Cing, bilat Forb	R F lat inf	R F lat inf	R F topectomy	2

Mégevand et al.

Accuracy of Electric Source Imaging in epilepsy

Supplementary Table 1

#	Gender	Age at evaluation	Age at onset	Classification	MRI findings	Surface spikes	ESI result	icEEG setup	icEEG spikes	icEEG seizure onsets	Surgery	Engel class
24	F	3	0	ETLE	tuberous sclerosis, R ATLR	R F-C = L F-T > R T-P	R mid T gyrus (post)	grid R F-P-T, grid R T-O, strips R Forb	R T > R P	R P-T	R T-O cortectomy	4
25	F	26	4	ETLE	L P post-infectious lesion	L P	L supramarginal gyrus	grid L F-P-T, strips L F, L T lat, L T basal, L F-P medial, depth L Hipp	L T-O = L P > L T basal	L T-O	L P lesionectomy	2
26	M	32	10	ETLE	normal	R F	R sup T gyrus (medial)	strips R F, R T lat, R T basal, R P, R T-O, R F-P medial	R F basal > R T basal	R F basal	NO	N/A
27	F	18	10	ETLE	normal	L F	L inf F gyrus (polar)	grid L F-T, grid L F medial, strips L Forb, L T basal, L P	L F ant	L F ant	L F ant lobectomy	2
28	M	10	4	ETLE	R P opercular and insular dysplasia	R F-P	R supramarginal gyrus	grid F-P-T R, strips R F-P dorsal, R F-P medial, R F polar, R T basal, R insula	R P	R P	R P lesionectomy	1
29	M	11	1	ETLE	bilat F and T cortical dysplasia, R F resection	R F-T	R inf F gyrus (pars opercularis)	grid R F, strips R F-P medial, R T basal, R F basal	R F inf post	R F lat inf post	R F topectomy	3
30	M	16	8	ETLE	L T-O cyst	L O	L cuneus	grid L T-O, strips L O medial, L T-O basal	L O basal medial	L O basal medial	L O lesionectomy	1
31	M	27	17	ETLE	R T-O polymicrogyria and dysplasia	R T-P-O > R T > L T	R O lingual gyrus (polar)	grid R T-O, depth bilat Forb, Amyg, Hipp	R T post-O inf > R Hipp post > L Hipp	R T post-O inf	R O cortectomy	3
32	M	39	20	ETLE	L HS, bilat periventricular heterotopia	L F-C	L mid F gyrus	depth L Amyg, L Hipp, L periventricular heterotopia, R Hipp, strips L F lat ant	L periventricular heterotopia > L F	L periventricular heterotopia	NO	N/A
33	F	15	0	ETLE	tuberous sclerosis	L P-O > L T	L angular gyrus	grid L T-F-P, strips L F, L T lat, L T basal	L P > L T lat sup > L T basal	L P	L T-P tuber resection and cortectomy	1
34	F	17	13	ETLE	resection R P abscess	R T > R C-P	R inf F gyrus (pars opercularis)	grid R F-P, strips R F-P medial, R T basal	R P sup > R F lat inf-P	R F lat inf-P	R P lesionectomy	3
35	M	22	3	ETLE	gliosis L P > R P, L F medial > R F medial	F bilat > F L	R sup F gyrus (medial)	grid L P-O-T, depth bilat Hipp, Cing, L Forb, L SMA, R P	L F medial > L T sup-F inf > L Hipp > R Hipp	(motor) L F medial (psychomotor) L P-O sup	L F medial lesionectomy	3
36	F	6	4	ETLE	ischemic sequelae L T-P-O, R P, L F-P, L F sup	R C = L F-C > C bilat > L T	L mid F gyrus	grid L F-P-T, strips L F, L F-P, L F-P medial, L T basal	L F medial > L T lat post sup > L P sup > L T polar > L F lat sup	L F medial and lat sup	R F medial lesionectomy	3
37	F	35	1	ETLE	normal	R T	R inf F gyrus (pars orbitalis)	strips R F lat, R T lat ant, R F medial, R P medial, depth R Hipp, R insula post	R F medial > R F lateral	R F medial	R F polar lobectomy	2
38	F	51	6	ETLE	resection R F dysplasia	no spikes, slowing R T	L inf F gyrus (pars orbitalis)	depth R F, bilat Amyg, Forb, Hipp	R T ant medial and lat > R F lat > L F lat	R F lat	R F lesionectomy	3

Abbreviations:

L=left, R=right, bilat=bilateral

F=frontal, C=central, T=temporal, P=parietal, O=occipital

ant=anterior, post=posterior, sup=superior, inf=inferior, lat=lateral

Hipp=hippocampus, parahipp=para-hippocampal gyrus, Amyg=amygdala, Forb=frontal orbital, Cing=cingular, SMA=supplementary motor area

HS=hippocampal sclerosis, ATLR=anterior temporal lobe resection

MTLE=medial temporal lobe epilepsy, LTLE=lateral temporal lobe epilepsy, ETLE=extra-temporal lobe epilepsy